A Study of the Role of the Maintained-Discharge Parameter in the Divisive Normalization Model of V1 Neurons

Tadamasa Sawada
School of Psychology
Higher School of Economics
20 Myasnitskaya Ulitsa
Moscow, Russia 101000
tada.masa.sawada@gmail.com

Alexander A. Petrov
Department of Psychology
Ohio State University
1827 Neil Avenue
Columbus, Ohio 43210
apetrov@alexpetrov.com

ABSTRACT

The divisive normalization model [Heeger, 1992] accounts successfully for a wide range of phenomena observed in single-cell physiological recordings from neurons in primary visual cortex (V1). Using mathematical analyses and simulation experiments, we investigated the role of the maintained-discharge (base firing rate) parameter in this model. We developed an implementation that can take grayscale images as inputs and applied it to the types of visual stimuli used in a comprehensive suite of published physiological studies. We found that three empirical phenomena are closely associated with the maintained-discharge parameter: (A) the existence of inhibitory regions in the receptive fields of simple cells in V1, (B) the supersaturation effect in the contrast sensitivity curves, and (C) the narrowing/widening of the spatial-frequency tuning curves when the stimulus contrast decreases. The model predicts two patterns of these phenomena: One possibility is that a neuron can show A, B, and widening (C); the other possibility is to show not-A, not-B, and narrowing (C). This interdependence is a potentially falsifiable prediction of the divisive normalization model.

Categories and Subject Descriptors

I.2.10 [**Artificial Intelligence**]: Vision and Scene Understanding; J.3. [**Computer Applications**]: Life and Medical Sciences—*Biology*

General Terms

Theory

Keywords

Primary visual cortex, Single-cell modeling, Divisive normalization

1. INTRODUCTION

Neurons in the primary visual cortex (area V1) of mammals have been extensively studied since the seminal studies of Hubel and Wiesel [16, 17]. There is ample evidence of systematic relationships between various properties of the retinal image and the firing rates of individual neurons in V1. A wealth of single-cell recording data in V1 have been accumulated since the 1960s [7] and a variety of computational and mathematical models have been proposed to account for the patterns in these data [3, 12].

Among those models, Heeger's [14] divisive normalization model has been very successful (see [4, 5, 14] for reviews). It functionally formulates a relation between visual stimuli and the response (firing rate) of an individual neuron. A general form of the model can be written as follows [25]:

$$R(I) = M\frac{\lfloor \beta + E_{tuned}(I) \rfloor^{n_N}}{\alpha^{n_D} + \sum_i w_i E_i(I)^{n_D}} \quad (1)$$

where M, n_N, n_D, α, and β are constants and I is a retinal image (see [2, 18] for analogous formulations). The parameters M, n_N, n_D, and α are positive. It is often assumed that $n_N = n_D = n$. The half-wave rectification operator $\lfloor E \rfloor$ equals E if $E > 0$ and 0 otherwise. The *stimulus drive* $E_{tuned}(I)$ in the numerator represents the classical receptive field of a neuron and its tuning in the orientation and spatial frequency domains. The model is tuned to a grating whose orientation is θ° and spatial frequency is f cycles/deg ($= \log_2 f$ octaves). The stimulus drive is formulated as:

$$E_{s:xyf\theta\phi}(I) = \iint I(X,Y) G_{xyf\theta\phi}(X,Y) \mathrm{d}X \mathrm{d}Y \quad (2)$$

where:

$$G_{xyf\theta\phi}(X,Y) = \exp\left(\frac{-\breve{X}^2 4\ln 2}{h_{\breve{X}}{}^2} + \frac{-\breve{Y}^2 4\ln 2}{h_{\breve{Y}}{}^2}\right)\sin\left(f\breve{Y} - \phi\right) \quad (3)$$

$$\begin{cases} \breve{X} = (Y-y)\sin\theta + (X-x)\cos\theta \\ \breve{Y} = (Y-y)\cos\theta - (X-x)\sin\theta \end{cases}$$

for a simple cell with preferred phase ϕ, and:

$$E_{c:xyf\theta}(I) = \sqrt{E_{s:xyf\theta 0^\circ}(I)^2 + E_{s:xyf\theta 90^\circ}(I)^2} \quad (4)$$

for a phase-invariant complex cell. Note that $h_{\breve{X}}$ and $h_{\breve{Y}}$ define the full-widths at half-height of the Gaussian envelope of the Gabor function $G_{xyf\theta\phi}(X,Y)$ and determine how sharply the stimulus drive is tuned to the grating [11].

.

BICT 2015, December 03-05, New York City, United States

DOI 10.4108/eai.3-12-2015.2262400

The *suppressive drive* $\Sigma_i w_i E_i(I)^{n_D}$ in the denominator represents the aggregated inhibitory influence from neurons with different tuning (cross-orientation suppression) and/or nearby receptive fields (surround suppression). Specifically, Equation 1 formalizes the hypothesis that the lateral interactions in V1 can be modeled in terms of divisive normalization.

Many of the past studies paid attention only to the exponent n and the semisaturation parameter α. In particular, a popular simplifying assumption is that $\beta = 0$, which neglects the potential role of this parameter. Our goal in this article is to explore this heretofore neglected aspect of the model. A positive value $\beta > 0$ is interpreted naturally as the maintained discharge of the neuron, defined as the firing rate when the retinal image I is in uniform gray. Empirically, physiological measurements of the maintained discharges of V1 neurons are usually low but non-zero [6, 15, 16, 22]. On the other hand, a negative value $\beta < 0$ in the context of the half-rectification operator in Equation 1 imposes a threshold on the stimulus drive. Such thresholding has been invoked to explain some phenomena observed in physiological experiments [13, 26, 28]. This shows that negative settings of β can affect the model predictions and opens the possibility that positive settings may affect the predictions too.

In this study, we conducted simulation experiments with a computer implementation of the divisive normalization model. The simulations were designed to investigate systematically the role of the parameter β in Equation 1.

2. SIMULATION EXPERIMENT

The divisive normalization model (Equation 1) was implemented in Matlab so that it can take a static grayscale image as input and produce a firing-rate response to this input. The model was calibrated and tested with a large set of stimuli taken from physiological experiments [24, 25] and the qualitative response patterns were compared with the corresponding patterns in the physiological data.

2.1 Model

The suppressive drive $\Sigma_i w_i E_i(I)^{n_D}$ in the denominator of Equation 1 is specified as follows:

$$\sum_i w_i E_i(I)^{n_D} = \sum_{x_i}^{N_X} \sum_{y_i}^{N_Y} \sum_{f_i}^{N_F} \sum_{\theta_i}^{N_\Theta} w_{x_i y_i} w_{f_i} w_{\theta_i} E_{c:xyf\theta}(I)^{n_D} \quad (5)$$

where:

$$\begin{cases} w_{x_i y_i} \propto \exp \frac{-((x_i-x)^2+(y_i-y)^2)4\ln 2}{{h_{R_w}}^2} \\ w_{\theta_i} \propto \exp\left(\kappa_{\Theta_w} \cos 2(\theta_i - \theta)\right) \\ w_{f_i} \propto \exp \frac{-(f_i-f)^2 4\ln 2}{{h_{F_w}}^2} \end{cases} \quad (6)$$

and h_{R_w}, κ_{Θ_w}, and h_{F_w} are constants specifying the widths of the pooling kernels w across space, orientations, and frequencies, respectively. This expression accounts for the cross-orientation [9] and surround [8] suppression of the neurons in V1. In cross-orientation suppression, the response of the neuron to a grating (signal) is suppressed by another grating (mask) superimposed on the signal within the classical receptive field (CRF). Surround suppression is the analogous effect when the mask is shown outside the CRF. It has been shown that the suppressions happen in wider ranges of the orientation and spatial-frequency domains than the excitatory tuning of the neuron [8, 9]. The response of the neuron is suppressed even by a grating whose orientation is orthogonal to the tuned orientation.

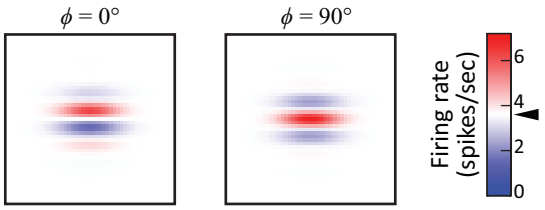

Figure 1: Maps of simple-cell receptive fields (RFs) in the model with $\beta = +0.03$ and two different phases ϕ. The RFs were measured with a light spot as a stimulus probe. The inhibitory sub-regions are depicted in blue. The response of the model became lower than its maintained discharge (3.6, indicated by the triangle ◀ on the color bar) when those regions are stimulated with the light spot. On the contrary, the response increased by stimulating the excitatory sub-regions (depicted in red).

The stimulus and the suppressive drives of the model are normalized so that their outputs equal 1.0 for a grating with the tuned frequency and the tuned orientation of the model, and with maximal contrast (= 1).

The model parameters in the simulation experiment were set as follows: $\beta = \pm 0.03$, $M = 40$, $n_N = n_D = 2.0$, $\alpha = 0.1$, $\theta = 90°$, $f = 2.0$ cycles/deg, $h_X = 0.63$ and $h_Y = 0.46$ deg, $\kappa_{\Theta_w} = 1.22$, $h_{F_w} = 2.0$ octaves, and $h_{R_w} = 1.0$. These settings reflect typical neurophysiological measurements [1, 2, 7, 27], prior modeling [14, 18], and calibration conventions.

2.2 Results

A comprehensive suite of physiological experiments were emulated using the computational model [24, 25]. The simulation results and the analysis below indicated that β plays a systematic role for the following three phenomena.

(A) First, β must be larger than 0 to account for the classic results of Hubel and Wiesel [16]. They observed that the response of a simple cell decreases below its maintained discharge when the inhibitory sub-region of the receptive field (Figure 1) is stimulated with a single spot of light. The effect of the suppressive drive $\Sigma_i w_i E_i(I)^{n_D}$ in Equation 1 is not strong enough by itself to account for this phenomenon when the stimulus is a single spot of light.

(B) It is often considered that the response increases monotonically as the contrast of the grating in the neuron's receptive field increases. However, at high stimulus contrasts the response of some V1 neurons has been observed to *decrease* as the contrast gets even higher [19, 21, 29]. Namely, the contrast sensitivity curves of those neurons are unimodal but are not monotonic (cf. Figure 2, solid line). This *supersaturation effect* can be emulated by the model only if the maintained discharge is high enough:

$$\beta > \frac{n_N}{n_D}(1 + \alpha^{n_D}) - 1 \quad (7)$$

To see why, consider a grating $g(c)$ with contrast c, the model's preferred orientation and frequency, and spatial ex-

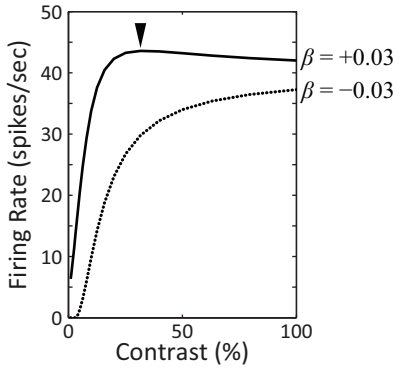

Figure 2: Contrast sensitivity curves of the model (complex cell) with $\beta = -0.03$ (dotted) and $\beta = +0.03$ (solid). The response of the model with $\beta = -0.03$ increased monotonically as the contrast of the grating increased. The response of the model with $\beta = +0.03$ showed a qualitatively different, nonmonotonic profile. The maximal response occurred in the middle of the range (32%, indicated by a triangle ▼) and slightly decreased at higher contrasts.

tent large enough to fill the entire receptive and surround-suppression fields. Then, from Equation 1 and our calibration conventions, the sensitivity curve for this grating is:

$$R(g(c)) = M\frac{\lfloor\beta + c\rfloor^{n_N}}{\alpha^{n_D} + c^{n_D}} \quad (8)$$

and its first derivative with respect to c is:

$$\frac{d}{dc}R(g(c)) = \frac{(c^{n_D}(n_N - n_D) - \beta n_D c^{n_D-1} + n_N\alpha^{n_D})}{M^{-1}(\alpha^{n_D} + c^{n_D})^2(\beta + c)^{1-n_N}} \quad (9)$$

for $\lfloor-\beta\rfloor \le c \le 1$. Note that $dR(g(c))/dc > 0$ at $c = 0$ and the contrast sensitivity curve is increasing at low contrasts. If Inequality 7 is satisfied, $dR(g(c))/dc < 0$ at $c = 1$. Then, the sensitivity function is decreasing at high contrasts and must have a local maximum between $\lfloor-\beta\rfloor$ and 1, exclusive. This is the supersaturation effect, and Inequality 7 is a sufficient condition for the effect.

(C) The tuning bandwidths of some V1 neurons in the spatial frequency domain become narrower while those of other V1 neurons become wider as the contrast of the grating decreases [1, 26]. It has been thought that this narrowing is caused by $\beta < 0$ (Figure 3) because the frequency tuning of the model mostly depends on its numerator. The bandwidth of the numerator of the model $\lfloor\beta + E_{tuned}(g(c))\rfloor^{n_N}$ becomes narrower as the contrast decreases if $\beta < 0$ and becomes wider if $\beta > 0$.

However, the tuning bandwidth of the model in the frequency domain also depends on its denominator. The denominator makes the bandwidth wider, and this widening effect becomes weaker as c decreases. Hence, the denominator explains the effect that the bandwidth of the model becomes narrower as c decreases, but not the opposite effect. Consider the tuning function of the denominator in the frequency domain. It is unimodal and has its maximum at the model's preferred frequency. Because of the division in Equation 1, a peaked denominator widens the bandwidth of the model as a whole, compared to the bandwidth of the numerator alone. This effect depends on c because the denominator, which includes the constant $\alpha^{n_D} > 0$, becomes wider as c decreases. Hence, if the bandwidth of a V1 neuron becomes narrower as c decreases, it can be explained by either the denominator or $\beta < 0$ (or both). On the other hand, if the overall bandwidth becomes wider as c decreases, it can be explained only by the numerator term ($\beta > 0$).

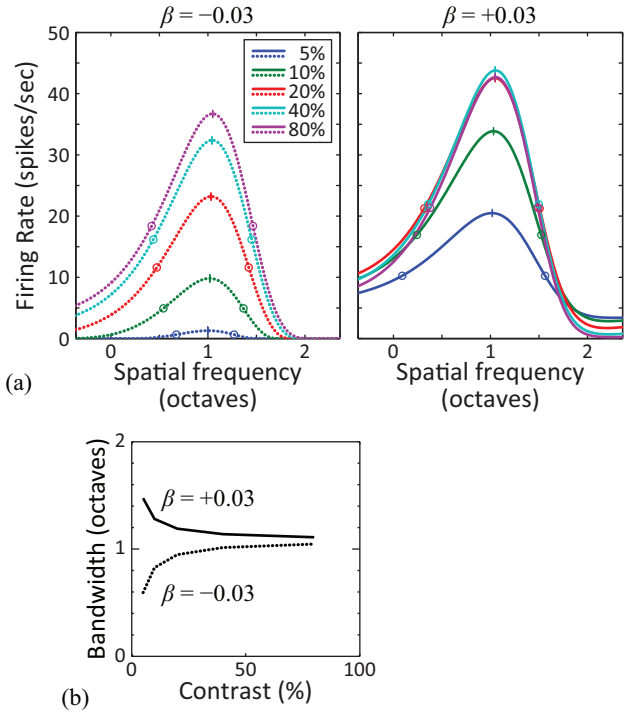

Figure 3: (a) Spatial frequency tuning functions of the model (complex cell) with $\beta = -0.03$ (left) and $\beta = +0.03$ (right) for different contrasts of the grating (depicted in different colors). The responses of the model at half height of the maximal responses for each contrast are indicated by circles. (b) Change of the tuning bandwidths (full width at half height) plotted as a function of the contrast of the grating.

Several physiological studies found an inconsistency between the tuning bandwidths estimated directly by probing the neuron with gratings of various orientations and frequencies, on the one hand, and those calculated from the 2D spatial pattern of excitatory and inhibitory sub-regions in the classical receptive field [20, 23, 28]. It has been thought that this phenomenon can be explained by thresholding the response of the neuron, which corresponds to $\beta < 0$ in Equation 1. However, the phenomenon is observed from the model with $n_N > 1$ and $n_D > 1$ [10] even if $\beta > 0$. The physiological data suggests that this condition of n_N and n_D is satisfied for many neurons in V1 [1, 2, 10, 27].

3. CONCLUSION

The results of the simulation experiment and the analysis on the divisive normalization model show how the parameter β affects phenomena A, B, and C listed above. To emulate both A and B, β must be sufficiently large. If β is too small, the model can emulate neither A nor B. At the same time, β affects whether the bandwidth of the model in the

frequency domain becomes wider or narrower as the contrast of the grating decreases (C). There is great diversity among V1 neurons and, to our knowledge, it has never been studied explicitly whether one and the same individual neuron can exhibit phenomena A, B, and C simultaneously.

The divisive normalization model predicts a pattern of interdependence among phenomena A, B, and C in neurons in primary visual cortex. This relationship is a potentially falsifiable prediction of the model.

4. ACKNOWLEDGMENTS

Supported by NIH Research Grant R21 EY022745-01.

5. REFERENCES

[1] D. G. Albrecht and D. B. Hamilton. Striate cortex of monkey and cat: Contrast response function. *Journal of Neurophysiology*, 48:217–237, 1982.

[2] L. Busse, A. R. Wade, and M. Carandini. Representation of concurrent stimuli by population activity in visual cortex. *Neuron*, 64:931–942, 2009.

[3] M. Carandini, J. B. Demb, V. Mante, D. J. Tolhurst, Y. Dan, B. A. Olshausen, J. L. Gallant, and N. C. Rust. Do we know what the early visual system does? *Journal of Neuroscience*, 25(46):10577–10597, 2005.

[4] M. Carandini and D. J. Heeger. Summation and division by neurons in visual cortex. *Science*, 264:1333–1336, 1994.

[5] M. Carandini and D. J. Heeger. Normalization as a canonical neural computation. *Nature Reviews Neuroscience*, 13(1):51–62, 2012.

[6] R. L. De Valois, D. G. Albrecht, and L. G. Thorell. Spatial frequency selectivity of cells in macaque visual cortex. *Vision Research*, 22:545–559, 1982.

[7] R. L. De Valois and K. K. De Valois. *Spatial Vision*. Oxford University Press, New York, 1988.

[8] G. C. DeAngelis, R. D. Freeman, and I. Ohzawa. Length and width tuning of neurons in the cat's primary visual cortex. *Journal of Neurophysiology*, 71(1):347–374, 1994.

[9] G. C. DeAngelis, J. Robson, I. Ohzawa, and R. D. Freeman. The organization of suppression in receptive fields of neurons in the cat's visual cortex. *Journal of Neurophysiology*, 68:144–163, 1992.

[10] J. L. Gardner, A. Anzai, I. Ohzawa, and R. D. Freeman. Linear and nonlinear contributions to orientation tuning of simple cells in the cat's striate cortex. *Visual Neuroscience*, 16:1115–1121, 1999.

[11] N. V. Graham. *Visual Pattern Analyzers*. Oxford University Press, New York, 1989.

[12] N. V. Graham. Beyond multiple pattern analyzers modeled as linear filters (as classical V1 simple cells): Useful additions of the last 25 years. *Vision Research*, 51:1997–1430, 2011.

[13] D. J. Heeger. Half-squaring in responses of cat striate cells. *Visual Neuroscience*, 9:427–443, 1992.

[14] D. J. Heeger. Normalization of cell responses in cat striate cortex. *Visual Neuroscience*, 9:181–197, 1992.

[15] D. H. Hubel. Single unit activity in striate cortex of unrestrained cats. *Journal of Physiology*, 147:226–238, 1959.

[16] D. H. Hubel and T. N. Wiesel. Receptive fields of single neurons in cat's visual cortex. *Journal of Physiology*, 148:574–591, 1959.

[17] D. H. Hubel and T. N. Wiesel. Receptive fields, binocular interaction, and functional architecture in the cat's visual cortex. *Journal of Physiology*, 160:106–154, 1962.

[18] L. Itti, C. Koch, and J. Braun. Revisiting spatial vision: Toward a unifying model. *Journal of the Optical Society of America A*, 17(11):1899–1917, 2000.

[19] C. Li and O. Creutzfeldt. The representation of contrast and other stimulus parameters by single neurons in area 17 of the cat. *Pflügers Archiv - European Journal of Physiology*, 401:304–314, 1984.

[20] S. Nishimoto, T. Ishida, and I. Ohzawa. Receptive field properties of neurons in the early visual cortex revealed by local spectral reverse correlation. *Journal of Neuroscience*, 26:3269–3280, 2006.

[21] J. W. Peirce. The potential importance of saturating and supersaturating contrast response functions in visual cortex. *Journal of VIsion*, 7(6:13):1–15, 2007.

[22] J. D. Pettigrew, T. Nikara, and P. O. Bishop. Responses to moving slits by single units in cat striate cortex. *Experimental Brain Research*, 6:373–390, 1968.

[23] D. L. Ringach. Spatial structure and symmetry of simple-cell receptive fields in macaque primary visual cortex. *Journal of Neurophysiology*, 88:455–463, 2002.

[24] T. Sawada and A. A. Petrov. A unified computational model of primary visual cortex: Consolidation of the scattered literature on simple and complex cells. *Journal of Vision*, 14(10):1189, 2014. (Abstract).

[25] T. Sawada and A. A. Petrov. A model oriented review of the simple and complex cells in V1. (Manuscript in preparation), 2015.

[26] M. P. Sceniak, M. J. Hawken, and R. Shapley. Contrast-dependent changes in spatial frequency tuning of macaque v1 neurons: effects of a changing receptive field size. *Journal of Physiology*, 88(3):1363–1373, 2001.

[27] G. Sclar, J. H. R. Maunsell, and P. Lennie. Coding of image contrast in central visual pathways of the macaque monkey. *Vision Research*, 30(1):1–10, 1990.

[28] Y. Tadmor and D. J. Tolhurst. The effect of threshold on the relationship between the receptive-field profile and the spatial-frequency tuning curve in simple cells of the cat's striate cortex. *Visual Neuroscience*, 3:445–454, 1989.

[29] C. W. Tyler and P. A. Apkarian. Effects of contrast, orientation and binocularity in the pattern evoked potential. *Vision Research*, 25:755–766, 1985.